UWB Planar Conical Horn-Shaped Self-Complementary Bow-Tie Antenna

A. Dastranj and M. Bornapour
Department of Electrical Engineering, Faculty of Engineering, Yasouj University, Yasouj, Iran,
dastranj@yu.ac.ir, mbornapour@yu.ac.ir
Corresponding author: Aliakbar Dastranj

***Abstract*- An ultra-wideband (UWB) self-complementary planar bow-tie antenna (SCPBTA) is proposed. The antenna consists of a printed conical horn-shaped (CHS) radiator and a counterpart CHS slot etched on a rectangular ground plane. The printed CHS radiator is connected directly to the 50Ω microstrip line by bending the end portion of the feed line. As a result, the antenna has a simple structure which does not require impedance matching networks. The antenna with a compact size of 32×38×1.2 mm^3 can cover UWB spectrum from 3.1 to 10.6 GHz. The simulation time- and frequency-domain results obtained from HFSS simulator package are verified by experimental measurements. Measured results for the reflection coefficient, far-field radiation patterns, radiation efficiency, gain, and group delay of the designed antenna over the UWB spectrum are presented and discussed. Measured data show good concordance with the numerical results. Also, the fidelity factor is calculated in both E- and H-plane by using CST Microwave Studio. The obtained results in both time- and frequency-domain indicate that the proposed SCPBTA is a good option for most practical UWB applications.**

***Index Terms*-** Bow-tie antenna, conical horn-shaped (CHS), impedance matching, UWB, SCPBTA, self-complementary

I. INTRODUCTION

Nowadays, ultra-wideband (UWB) wireless communication technology has received widespread concentration due to its great capacity, high data rates, low operating power level and low complexity. The modern UWB wireless communication systems need miniaturized and wideband antennas with high radiation efficiency. These mechanical and electromagnetic specifications have required the development of novel antenna structures [1].

Over the past decade, to satisfy the UWB wireless communication technology requirements, various configurations of printed antennas including planar monopole antennas [2-7], quasi-Yagi antennas [8, 9], and printed dipole antennas [10, 11] have been reported. In addition, as a kind of

Manuscript received 15-May-2018 and revised 7-Nov.-2018,
Accepted on 9- Jan.-2019
P- ISSN: 2322-4088
E- ISSN: 2322-3936

printed antenna, the bow-tie antenna has become one of the main forms of wideband antennas. Bow-tie structures presented in the literature can be given as slot [12], double-sided [13], self-complementary [14], and self-grounded [15]. Various bowtie antennas fed by coaxial line [16], coplanar waveguide [17] and stripline [18], were designed for many applications, such as ground penetrating radar [19] and pulse antennas [20].

Printed bow-tie antennas have been greatly utilized in UWB communication and phased array systems due to their wide operational bandwidths [21]. In the past few years, to satisfy the UWB communication systems requirements, several researches on bow-tie antennas have been reported [22-34]. In [22], a monolayer bow-tie slot antenna with triband operation was presented. An improved bow-tie antenna with reduced metallization based on the phenomenon that the majority of the current density was confined towards the edges of the patch was proposed in [23]. In [24], a directional wideband self-grounded bow-tie antenna with a volume of 54×58×24 mm^3can cover a bandwidth of 3–15 GHz. A multiband Koch-like sided fractal bow-tie dipole antenna was reported in [25]. A low-profile bow-tie antenna with multiband operation was presented for multistandard applications [26]. In [27], a microstrip balun fed wideband printed modified bow-tie antenna, consisting of rounded T-shaped slot loaded bow arms was proposed. In [28], a directive bow-tie antenna with an impedance bandwidth of 117% (0.85-3.25 GHz) for three-dimensional microwave imaging systems was designed. In [29], a CPW-fed bow-tie slot antenna with a dual-band function was presented. It can provide two operating bandwidths of 1450 MHz (about 32.8% centred at 4.43 GHz) and 3500 MHz (about 37.8% centred at 9.25 GHz). A new bow-tie slot antenna was implemented in [30]. By replacing a conventional narrow rectangular slot with a bow-tie shaped slot, unidirectional radiation characteristics over a bandwidth of 1.03 GHz (9.4%) were obtained. In [31], a bow-tie antenna with frequency-reconfigurable behaviour was presented. It can be adjusted to cover the frequency ranges of 2.2–2.53, 2.97–3.71, or 4.51–6 GHz with desirable radiation characteristics. Recently, a new asymmetric coplanar waveguide (ACPW)-fed bow-tie antenna with different slot lengths was presented [32]. By adjusting the length of one ACPW slot, a working frequency band of 2.76-8.1 GHz was obtained. In [33], a fractal artificial magnetic conductor structure was designed as the ground plane of a printed bow-tie antenna for gain enhancement and low profile. The antenna can cover a bandwidth from 1.64 to 1.94 GHz. In [34], by using a pair of tilted bow-tie radiators fed through substrate integrated waveguide feed-line, a millimetre-wave bow-tie antenna with an impedance bandwidth of 57–64 GHz was designed.

It should be pointed out that the input impedance of the bow-tie antenna is 300 Ω [35]. Therefore, to feed this type of antenna, it is necessary to design an impedance matching network such as multi-section stub with different widths and balun transformer for matching the bow-tie to the 50 Ω microstrip feed line. On the other hand, the matching section results in complexity in the antenna geometry.

To overcome the aforementioned problem and design a simple UWB antenna, a new self-complementary planar bow-tie antenna (SCPBTA) is proposed in this work. The SCPBTA comprises a printed conical horn-shaped (CHS) radiator and a counterpart CHS slot etched on a rectangular ground plane. The printed CHS patch is connected directly to the 50Ω microstrip line by bending the end portion of the feed line. Consequently, the antenna has a simple structure which does not require matching sections. The antenna has an overall size of 32×38×1.2 mm^3 while can provide a working frequency band of 3.1-10.6 GHz (UWB spectrum). The simulation time- and frequency-domain results obtained from HFSS simulator package were verified by experimental measurements. Experimental outcomes show good concordance with the numerical outcomes. Compared to recent designs reported in [29-32], the proposed antenna is easier in structure and fabrication while it provides a wider bandwidth and smaller size. The experimental outcomes indicate that the SCPBTA is a competent option for use in UWB communication or phased array systems.

II. ANTENNA DESIGN

The main goal of this research is to design a novel and simple model of bow-tie antenna which does not require impedance matching network and it is extremely comfortable for connecting to 50Ω coaxial connector. To do this, the self-complementary antenna theory [36] is used. The novelty of the proposed design lies in its simple configuration and simplicity to obtain the desired antenna characteristics in both time- and frequency-domain. Fig. 1 illustrates the geometry and design parameters of the proposed SCPBTA. The SCPBTA is printed on FR4 substrate of a permittivity of 4.4, a conductor loss (tan δ) of 0.02, and dimensions of 32×38×1.2 mm^3 (length × width× thickness) . As it can be observed in Fig. 1, the proposed SCPBTA comprises a printed CHS radiator and a counterpart CHS slot etched on the rectangular ground plane. The printed CHS patch is connected directly to the 50Ω microstrip line by bending the end portion of the feed line. Consequently, the antenna has a simple structure which does not require matching sections. Notice that the proposed design is extracted from the initial antenna structure presented in Fig. 2. The design of initial antenna is the first stage in the design procedure, which comprises a common triangular-shaped radiator and a counterpart triangular slot etched on the ground plane. The lower frequency of the working band (unit in GHz) can be calculated approximately from the following formula [37]:

$$f_L = \frac{7.2}{\left[\left(\frac{\sqrt{3}L_p}{2}\right) + \left(\frac{L_p}{4\pi}\right) + W_r\right]\left(\frac{\sqrt{1+\varepsilon_r}}{2}\right)} \quad (1)$$

Where Lp and Wr are length of triangular patch and width of bended portion of the fed line, respectively (see Figs. 1 and 2). In fact, the above equation calculates the frequency for the triangular monopole antenna which is the closer shape to the proposed SCPBTA [37]. In order to satisfy the lower frequency of the UWB spectrum, 3.1 GHz, the values of Lp and Wr obtained from (1), are 13

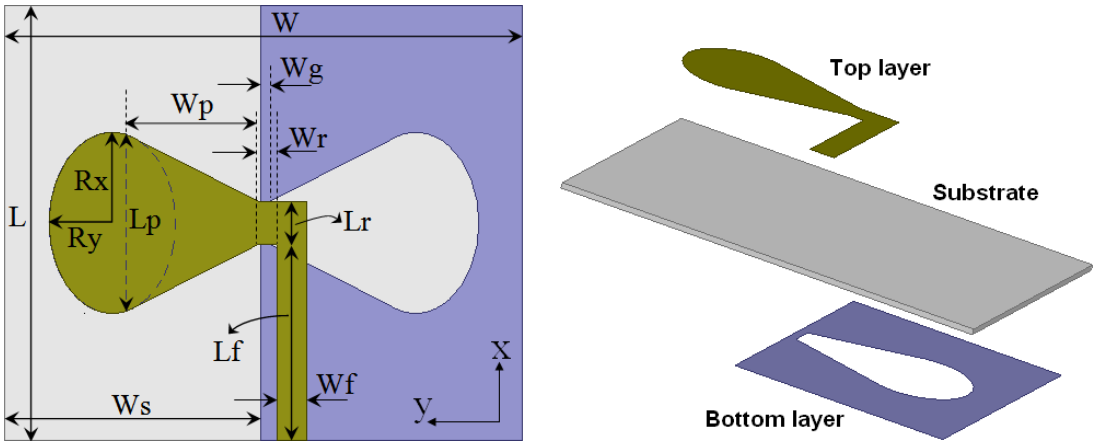

Fig. 1. Antenna geometry and design parameters.

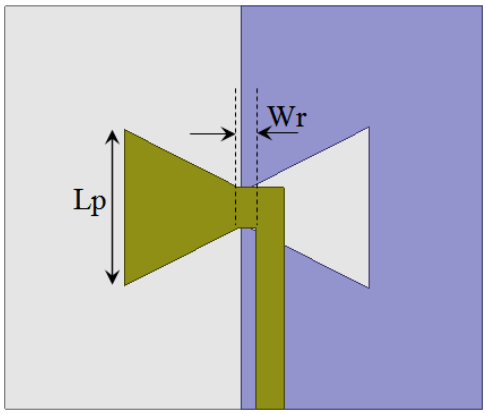

Fig. 2. Initial antenna structure (the other geometrical parameters are as presented in Fig.1).

mm and 1.4 mm, respectively. The other geometrical parameters of the antenna were optimized using Ansoft HFSS. Fig. 3 shows the corresponding simulated impedance matching curves of the initial design and the proposed SCPBTA. It is seen that the initial design covers the frequency range of 3.8 to 7.2 GHz (defined by -10-dB reflection coefficient), while it has two resonance frequencies which occur at 4.4 and 6.5 GHz, respectively. It is seen that the lower and higher band edge frequencies are shifted from 3.8 to 3.1GHz and 7.2 to 10.6 GHz, respectively, which leads to an impedance bandwidth from 3.1 to 10.6 GHz (UWB operation) for $|S_{11}| < -10$ dB. As shown in Fig. 3, the third resonance frequency of the SCPBTA is occurred at 8.8 GHz. the optimal dimensions of the SCPBTA are as follows: W = 38 mm, L = 32 mm, Ws = 18.8 mm, Wf = 2.2 mm, Lf = 14.4 mm, Lr = 3.2 mm, Wg = 0.7 mm, Wp = 9.4 mm, Rx = 6.65 mm, and Ry = 4.66 mm.

In order to more investigate the influence of the CHS radiator and the counterpart CHS slot on the impedance characteristic of the antenna, the surface current distribution on the antenna radiator and

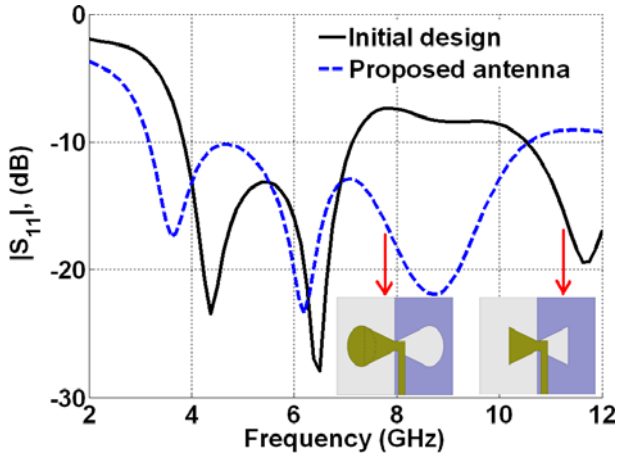

Fig. 3. Numerical reflection coefficients of the initial and proposed antennas versus frequency.

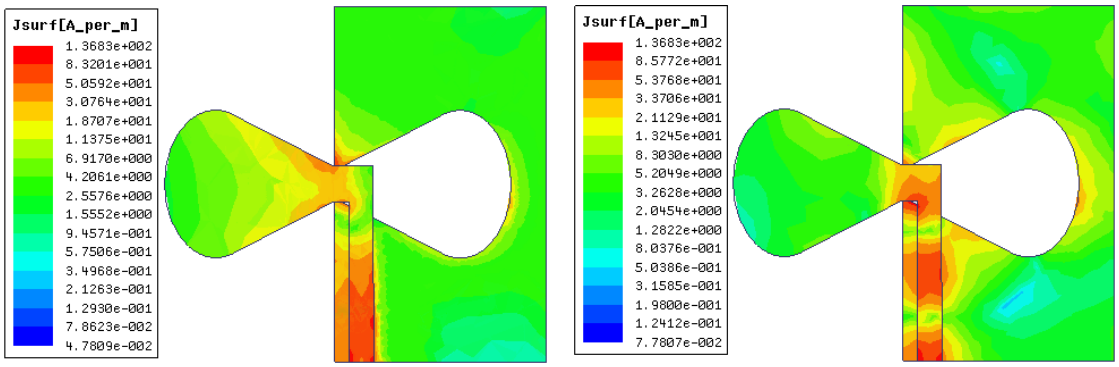

(a) (b)

Fig. 4. Simulated Surface current distribution of the proposed antenna, (a) at 3.5 GHz, (b) at 9 GHz.

ground plane at 3.5 and 9 GHz is presented in Fig. 4. As shown in Fig. 4(a), the current distribution at the first resonant frequency, 3.5 GHz, is concentrated on the CHS radiator, while at the third resonant frequency, 9 GHz, current distribution is mainly concentrated around the counterpart CHS slot (see Fig. 4(b)). This means the CHS radiator and the counterpart CHS slot affect impedance characteristic at low and high frequencies, respectively.

Numerical Parametric analysis was performed to understand the influence of the antenna physical dimensions on the impedance bandwidth. Through numerous simulations, it was found that the main geometrical parameters Wr, Lr, and the ellipticity ratio (Ry/Rx) considerably affect the antenna reflection coefficient. The criterion for selecting these parameters is to cover UWB spectrum from 3.1 to 10.6 GHz. The influence of Wr and Lr, on the antenna impedance characteristic is depicted in Fig. 5 (highlighted with the green loops) while the other physical dimensions are unchanged. It is seen in Fig. 5 (a) that by increasing Wr from 0.6 to 2.2 mm, the lower frequency of the bandwidth changes from 3.3 to 3 GHz which is compatible with (1). However, the antenna reflection coefficient increases

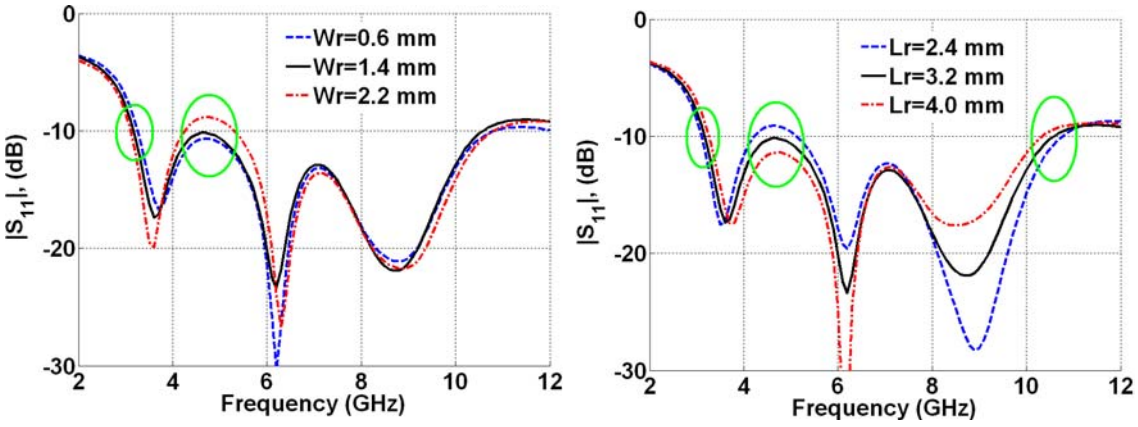

(a) (b)

Fig. 5. Influence of Wr and Lr on the impedance bandwidth of the antenna, (a) Wr, (b) Lr.

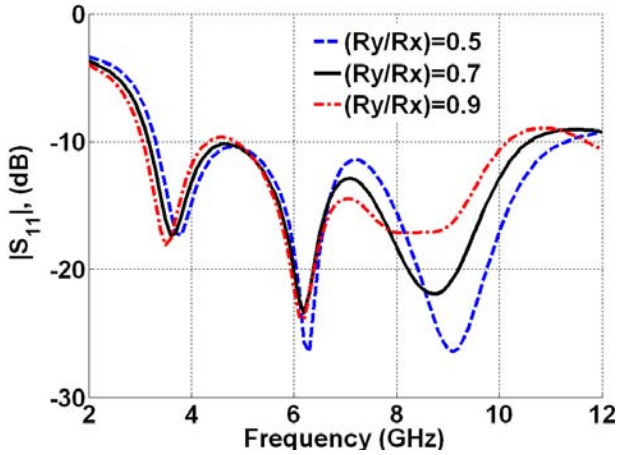

Fig. 6. Influence of Ry/Rx on the impedance bandwidth of the antenna.

in 4–6 GHz frequency range. As shown in this figure, the selected value of Wr=1.4 mm leads to UWB characteristic for the antenna. The influence of Lr on the impedance bandwidth is presented in Fig. 5(b). As depicted in this figure, by increasing Lr from 2.4 to 4.0 mm, the antenna reflection coefficient improves in 4–6 GHz frequency range, while the higher band edge frequency closes to the lower band edge frequency which leads to a narrower impedance bandwidth. Also, the impedance bandwidth of the antenna can be controlled by the radii of elliptical sections, Rx, Ry. Fig. 6 illustrates the influence of the ellipticity ratio, (Ry/Rx), on the antenna impedance bandwidth. In this case, the other physical dimensions of the antenna are unchanged and Rx is fixed at 6.65 mm. As it can be observed, for Ry/Rx=0.5, the antenna provides a bandwidth form 3.3 to 11.3 GHz, while for Ry/Rx=0.9 the antenna reflection coefficient increases at the frequencies about 4.6 GHz. Fig. 6 shows that selecting the optimal value of Ry/Rx=0.7 (Rx=6.65 mm, Ry=4.66 mm) leads to UWB operation. The optimal value of Ry/Rx=0.7 is obtained by optimization process via Ansoft HFSS.

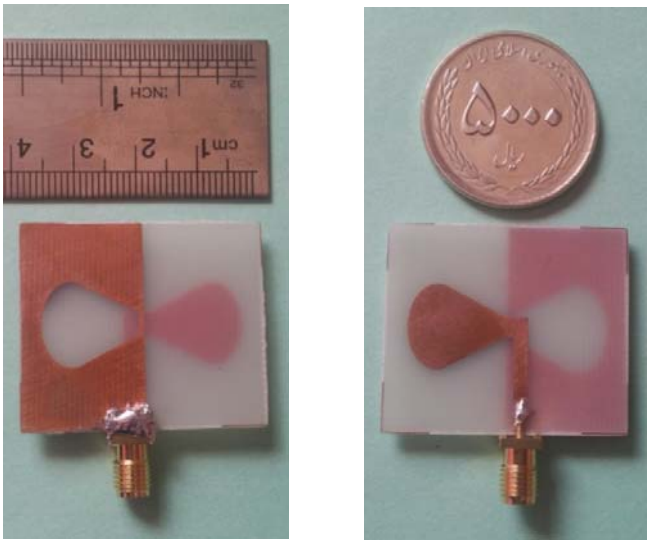

Fig. 7. Fabricated SCPBTA (left: bottom, right: top).

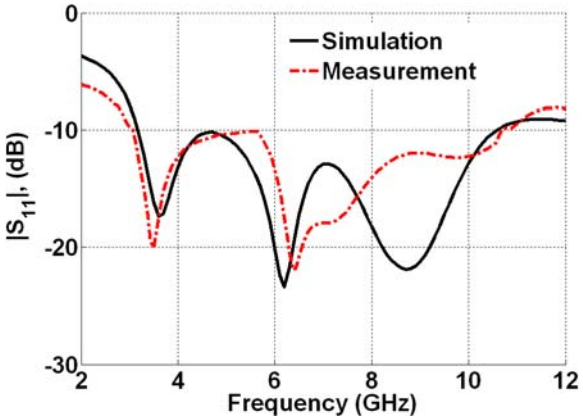

Fig. 8. Numerical and experimental reflection coefficients versus frequency.

III. SIMULATED AND MEASURED RESULTS

In order to validate the numerical outcomes obtained by Ansoft HFSS, the designed SCPBTA was constructed and tested. The fabricated antenna is shown in Fig. 7. In the following, the experimental outcomes are given, discussed, and compared with the numerical results.

A. Frequency-domain results

Fig. 8 presents the comparison of experimental and numerical reflection coefficients of the SCPBTA. The slight difference between the experimental result and numerical data is due to measurement errors and test equipment. Both measured and simulated outcomes indicate that the SCPBTA features desirable impedance matching over the whole UWB spectrum, from 3.1 to 10.6 GHz. However, to determine the overall bandwidth of the antenna, other radiation parameters of the

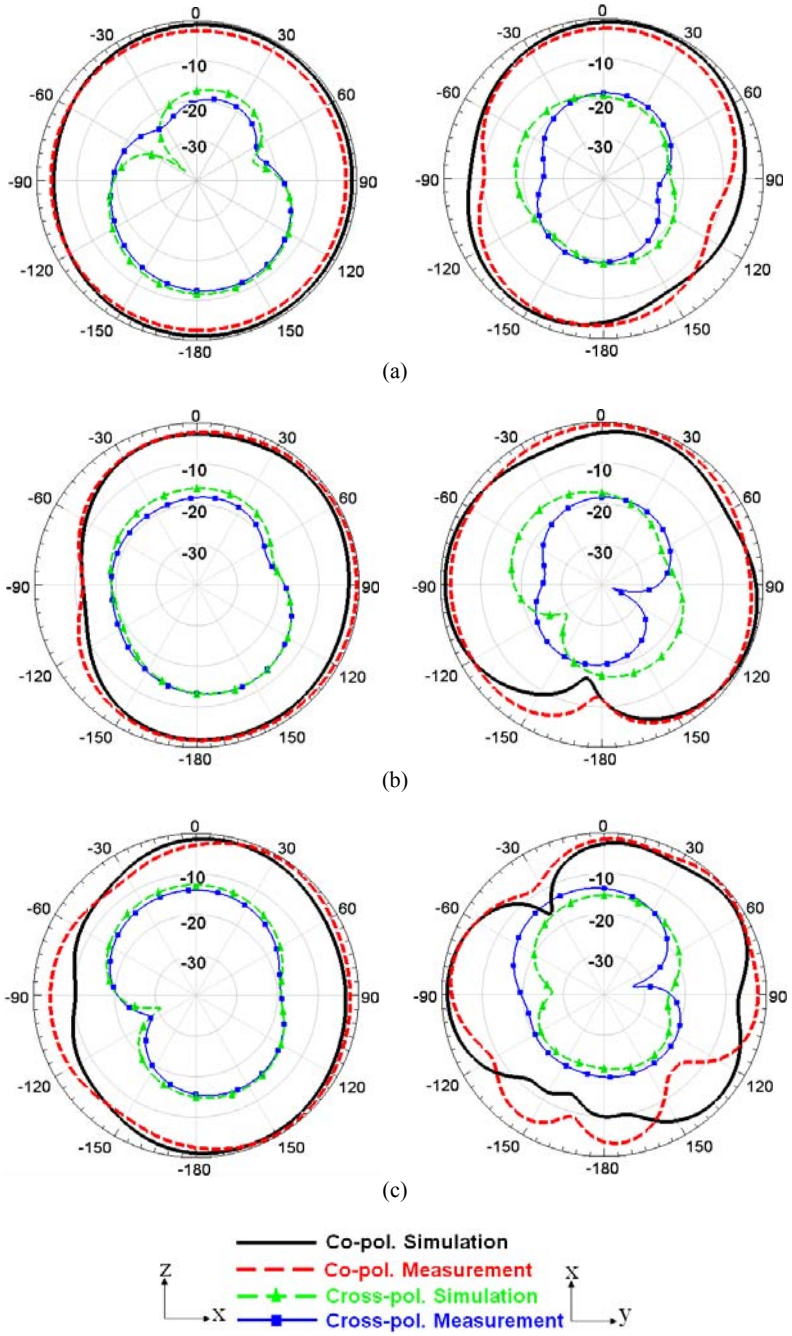

Fig. 9. Experimental and numerical co-and cross-polar far-field patterns of the SCPBTA (left: H- plane, right: E- plane), (a) at 4 GHz, (b) at 7 GHz, (c) at 10 GHz.

antenna such as far-field patterns, radiation efficiency, and gain must also be carefully examined over the entire frequency band [38].The radiation patterns were measured at different frequencies. For brevity, the numerical and experimental H (x-z)-and E (x-y)-plane patterns at only 4, 7, and 10 GHz are compared in Fig. 9. A good concordance between the numerical and experimental outcomes is seen. It is observed that the SCPBTA provides nearly omnidirectional patterns specifically in the H-plane. As

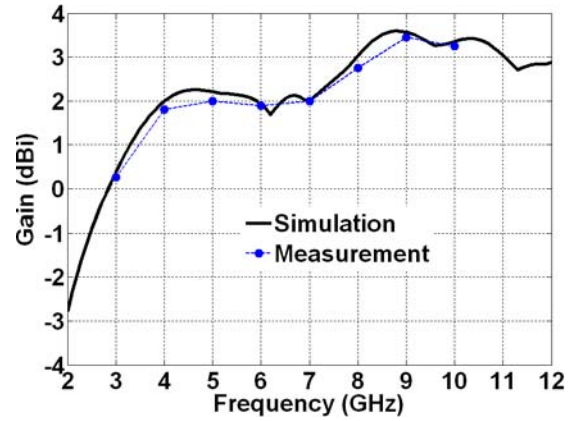

(a)

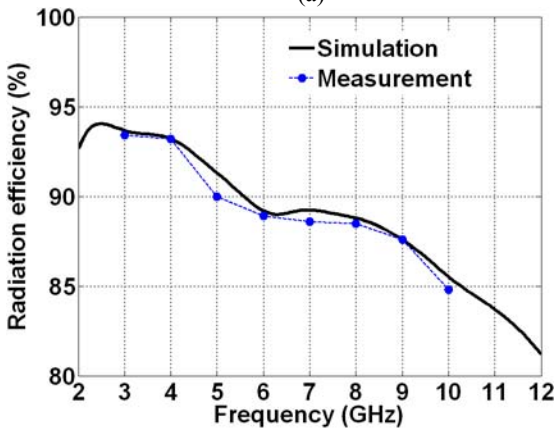

(b)

Fig. 10. Numerical and experimental radiation parameters of the SCPBTA versus frequency, (a) gain, (b) radiation efficiency.

shown in this figure, the magnitude of cross-polarized component is acceptable over the entire frequency band.

Fig. 10 plots the experimental and numerical gain and radiation efficiency of the proposed SCPBTA versus frequency. Fig. 10 (a) illustrates that the measured gain has an average value of 2.18 dBi. Based on the measured result, the maximum value of the antenna gain is 3.45 dBi which occurs at 9 GHz. Also, the gain variation is less than 3.2 dBi over the UWB spectrum. Notice that the measured gain of the SCPBTA is moderate at the desired frequency range respecting the compact size and omnidirectional behaviour of the antenna. Besides, as shown in Fig. 10 (b), the fabricated antenna can provide desirable radiation efficiency of greater than 84% over the frequency range of 3-10 GHz. The antenna radiation efficiency is also desirable considering the FR4 substrate with loss tangent of 0.02. The antenna radiation efficiency was computed based on the measured data using the following equation.

$$\text{radiation efficiency} = \frac{\mathrm{G}}{(1-|\Gamma|^2)\mathrm{D}} \tag{2}$$

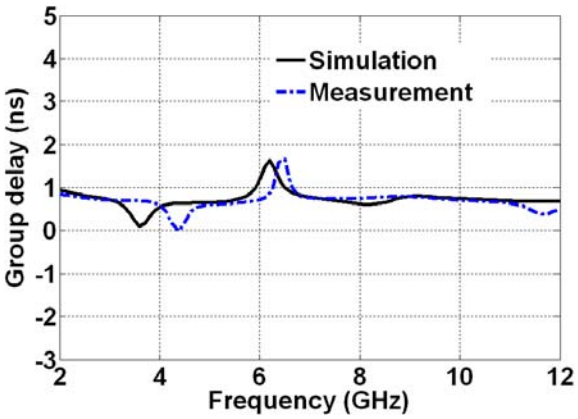

Fig. 11. Experimental and numerical group delay outcomes for the SCPBTA versus frequency.

where G, D, and Γare gain, directivity, and the reflection coefficient of the antenna, respectively [39]. Notice that, directivity and gain were measured in the direction of maximum radiation.

B. Time-domain results

To analyse the time-domain characteristic of the designed SCPBTA, group delay and fidelity factor parameters are investigated. These time-domain characteristics determine the signal distortion which an antenna adds to its input signal. Notice that the signal distortion reduces signal-to-noise ratio and increases bit error rate in communication systems. In a wideband communication system, the group delay is one of the important characteristics. This parameter can cause pulse distortion, and consequently signal to noise or bit error degradation. In order to provide desirable time-domain behaviour, constant group delay is required over the entire working band. Fig. 11 presents the experimental and numerical group delay curves of the SCPBTA for face-to-face case. To investigate the group delay, the distance between the receiving and transmitting antennas was selected as 500 mm. As shown in Fig. 11, the total variation of the measured group delay is limited to less than 1.7 ns over the whole working band. The results indicate that the fabricated SCPBTA has an acceptable time domain characteristic. Although not shown, similar results for side-by-side configuration were obtained. As shown in Fig. 11, the peaks of the group delay are occurred at 3.8 GHz and 6.2 GHz which are related to the first and second resonant frequencies of the antenna (3.8 GHz and 6.2 GHz) at Fig. 8. The difference between the peaks of the simulated and measured curves is due to the measurement errors and test equipment.

To obtain the real-time response of the antenna, two antennas were put face-to-face at a distance of 500 mm between them. An UWB pulse synthesized in the vector network analyzer to cover the band 3.1–10.6 GHz was transmitted from the first antenna, and the received pulse by the second antenna was measured. The result is shown in Fig. 12 (a real-time photograph), where amplitudes of the transmitted and received pulses were normalized to have a peak equal to 1. It is clear from Fig. 12

that the antenna is efficient in the UWB pulse operation where the received pulse has a low distortion.

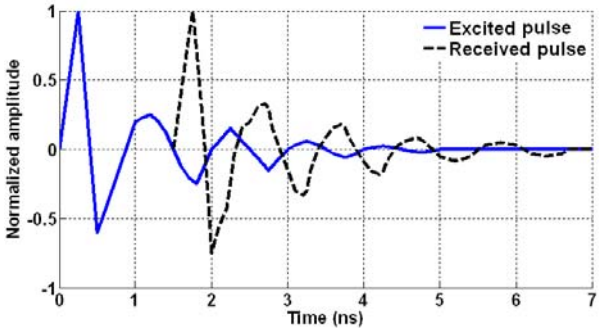

Fig. 12. Time-domain response of the antenna.

Table I. Calculated fidelity factor of the antenna

Angle (degrees)	fidelity factor	
	E-plane	H-plane
0	0.89	0.90
15	0.87	0.89
30	0.88	0.91
45	0.85	0.87
60	0.84	0.85
75	0.82	0.82
90	0.80	0.81

The fidelity factor is generally preferred as a time domain performance parameter. In the last step of this work, fidelity factor is calculated by using CST Microwave Studio. By utilizing the approach presented in [40], the input pulse is delivered to the antenna, and the electric component in the far-field region is received via seven virtual probes. The distance between the transmitting antenna and the probes maintains at 500 mm. The fidelity factor is calculated in both E- and H-plane. In each plane, seven probes are located with the angle equal to 0°, 15°, 30°, 45°, 60°, 75°, and 90°, respectively. The calculated fidelity factor for both planes is presented in Table I. As it can be observed, the fidelity factor in both planes is more than 0.8, making the antenna suitable for most practical UWB applications.

Compared to recent designs reported in [29-32], the proposed antenna features broader overall bandwidth and smaller size, simultaneously, while it is easier in structure and fabrication. The operating frequency ranges of the antennas presented in [29-32] are 0.85-3.25 GHz, 9.7-10.7 GHz, 4.51-6 GHz, and 2.76-8.1 GHz, respectively. However, the designed antenna can cover UWB spectrum from 3.1 to 10.6 GHz. It should be noted than the time-domain characteristics of the bow-tie antennas in [29-32], were not presented and discussed. The experimental results in time as well as frequency domain prove that the SCPBTA is an excellent option for UWB wireless systems and phased array applications.

IV. CONCLUSION

Based on the self-complementary antenna theory, a new and simple SCPBTA for UWB applications has been presented. The antenna consists of a printed CHS radiator and a counterpart CHS slot etched on the ground plane. The printed CHS patch is connected directly to the 50Ω microstrip line by bending the end portion of the feed line. Consequently, the antenna has a simple structure which does not need impedance transformer sections. The antenna has a total size of 32×38×1.2 mm^3 and covers UWB spectrum from 3.1 to 10.6 GHz. The experimental and numerical performance parameters of the designed SCPBTA in both time- and frequency-domain have been presented and discussed. Compared to a number of recent designs reported in open literature, the proposed antenna is easier in structure and fabrication while it provides a wider bandwidth and smaller size. The measured outcomes show that the SCPBTA is a competent option for use in UWB communication or phased array systems.

REFERENCES

[1] C.-Y. Huang, C.-C. Lin, and W.-F. Chen, "Multiple band-stop bow-tie slot antennas for multiband wireless systems," *IET Microw. Antennas Propag.,* vol. 2, no. 6, pp. 588–593, September 2008.

[2] S. A. Rezaeieh, A. MAbbosh, and M. A. Antoniades, "Compact CPW-fed planar monopole antenna with wide circular polarization bandwidth," *IEEE Antennas Wireless Propag. Lett.,* vol. 12, pp. 1295-1298, September 2013.

[3] O. Ahmed and A. R. Sebak, "A printed monopole antenna with two steps and a circular slot for UWB applications," *IEEE Antennas Wireless Propag. Lett.,* vol. 7, pp. 411–413, June 2008.

[4] H. Oraizi and S. Hedayati, "Miniaturized UWB monopole microstrip antenna design by the combination of GiusepePeano and Sierpinski carpet fractals," *IEEE Antennas Wireless Propag. Lett.,* vol. 10, pp. 67–70, January 2011.

[5] A. M. Abbosh and M. E. Bialkowsky, "Design of ultrawideband planar monopole antennas of circular and elliptical shape," *IEEE Trans. Antennas Propag.,* vol. 56, no. 1, pp. 17-23, January 2008.

[6] M. Koohestani and M. Golpour, "U-shaped microstrip patch antenna with novel parasitic tuning stubs for ultra wideband applications," *IET Microw. Antennas Propag.,* vol. 4, no. 7, pp. 938–946, July 2010.

[7] A. A. Dastranj, "Very small planar broadband monopole antenna with hybrid trapezoidal-elliptical radiator," *IET Microw. Antennas Propag.,* vol. 11, no. 4, pp. 542-547, March 2017.

[8] N. Kaneda, W. Deal, Y. Qian, R. Waterhouse, and T. Itoh, "A broad-band planar quasi-Yagi antenna," *IEEE Trans. Antennas Propag.,* vol. 50, no. 8, pp. 1158–1160, August 2002.

[9] W. Deal, N. Kaneda, J. Sor, Y. Qian, and T. Itoh, "A new quasi-Yagi antenna for planar active antenna arrays," *IEEE Trans. Microwave Theory Tech.,* vol. 48, no. 6, pp. 910–918, June 2000.

[10] G.-Y. Chen and J.-S. Sun, "A printed dipole antenna with microstrip tapered F," *Microw. Opt. Technol. Lett.,* vol. 40, no. 4, pp. 344–346, February 2004.

[11] G. Zheng, A. A. Kishk, A. B. Yakovlev, and A. W. Glisson, "Simplified feed for a modified printed Yagi antenna," *Electronics Letters,* vol. 40, no. 8, pp. 464–466, April 2004.

[12] A. Mehdipour, K. M. Aghdam, R. Faraji-Dana, and A. R. Sebak, "Modified slot bow-tie antenna for UWB applications," *Microw. Opt. Technol. Lett.,* vol. 50, no. 2, pp. 429–432, February 2008.

[13] T. Karacolak, and E.Topsakal, "A double-sided rounded bow-tie antenna (DSRBA) for UWB communication," *IEEE Antennas Wireless Propag. Lett.,* vol. 5, pp. 446–449, October 2006.

[14] K. H. Sayidmarie and Y. A. Fadhel, "A planar self-complementary bow-tie antenna for UWB application," *Progress in Electromagnetics Research C,* vol. 35, pp. 253-267, 2013.

[15] S. Mansouri-Moghaddam, P.-S. Kildal, A. A. Glazunov, J. Yang, and M. Gustafsson, "A self-grounded dual-polarized wideband bowtie with improved MIMO performance in Random-LOS," *IEEE International Symposium on Antennas and Propagation (APSURSI), Fajardo, Puerto Rico,* 26 June-1 July 2016, pp. 531 – 532.

[16] A. A. Lestari, A. G. Yarovoy, and L. P. Ligthart, "RC-loaded bow-tie antenna for improved pulse radiation," *IEEE Trans. Antennas Propag.,* vol. 52, no. 10, pp. 2555–2563, October 2004.

[17] A. Eldek, A. Z. Elsherbeni, and C. E. Smith, "Characteristics of bow-tie slot antenna with tapered tuning stubs for wideband operation," *Progress In Electromagnetics Research*, vol. 49, pp. 53–69, 2004.

[18] *Y.-D. Lin, and S.-N. Tsai, "Analysis and design of broadside-coupled striplines-fed bow-tie antennas," IEEE Trans. Antennas Propag.*, vol. 46, no. 3, pp. 459–460, March 1998.

[19] D. Uduwawala, M. Norgren, P. Fuks, and A. W. Gunawardena, "A deep parametric study of resistor-loaded bow-tie antennas for ground penetrating radar applications using FDTD," *IEEE Trans. Geoscience Remote Sensing*, vol. 42, no 4, pp. 732–742, April 2004.

[20] C. Waldschnidt and K. D. Palmer, "Loaded wedge bow-tie antenna using linear profile," *Electronics Letters,* vol. 37, pp. 208–209, 2001.

[21] A. A. Eldek, A. Z. Elsherbeni, and C. E. Smith, "Wide-band modified printed bow-tie antenna with single and dual polarization for C- and X-band applications," *IEEE Trans. Antennas Propag.,* vol. 53, no. 9, pp. 3067–3072, September 2005.

[22] Y. C. Chen, S. Y. Chen, and P. Hsu, "A compact triband bow-tie slot antenna fed by a coplanar waveguide," *IEEE Antennas Wireless Propag. Lett.*, vol. 9, pp. 1205–1208, December 2010.

[23] A. C. Durgun, C. A. Balanis, C. R. Birtcher, and D. R. Allee, "Design, simulation, fabrication and testing of flexible bow-tie antennas," *IEEE Trans. Antennas Propag*., vol. 59, no. 12, pp. 4425-4435, December 2011.

[24] J. Yang and A. Kishk, "A novel low-profile compact directional ultrawideband antenna: the self-grounded bow-tie antenna," *IEEE Trans. Antennas Propag*., vol. 60, no. 3, pp. 1214–1220, March 2012.

[25] D. Li and J.-F. Mao, "A koch-like sided fractal bow-tie dipole antenna," *IEEE Trans. Antennas Propag.,* vol. 60, no. 5, pp. 2242-2251, May 2012.

[26] M. A. Antoniades and G. V. Eleftheriades, "Multiband compact printed dipole antennas using NRI-TL metamaterial loading," *IEEE Trans. Antennas Propag.,* vol. 60, no. 12, pp. 5613–5626, December 2012.

[27] O. Yurduseven, D. Smith, and M. Elsdon, "Printed slot loaded bow-tie antenna with super wideband radiation characteristics for imaging applications," *IEEE Trans. Antennas Propag.,* vol. 61, no. 12, pp. 6206-6210, December 2013.

[28] H. W. Liu, X. Zhan, S. Li, J. H. Lei, and F. Qin, "Dual-band bow-tie slot antenna fed by coplanar waveguide," *Electronics Letters,* vol. 50, no. 19, pp. 1338-1340, September 2014.

[29] M. Jalilvand, X. Li, J. Kowalewski, and T. Zwick, "Broadband miniaturized bow-tie antenna for 3D microwave tomography," *Electronics Letters*, vol. 50, no. 4, pp. 244-246, February 2014.

[30] S. Mukherjee, A. Biswas, and K. V. Srivastava, "Broadband substrate integrated waveguide cavity-backed bow-tie slot antenna," *IEEE Antennas Wireless Propag. Lett.,* vol. 13, pp. 1152-1155, June 2014.

[31] T. Li, H. Zhai, X. Wang, L. Li, and C. Liang, "Frequency-reconfigurable bow-tie antenna for Bluetooth, WiMAX, and WLAN applications," *IEEE Antennas Wireless Propag. Lett.,* vol. 14, pp. 171-174, February 2015.

[32] L. Xu, L. Li, and W. Zhang, "Study and design of broadband bow-tie slot antenna fed with asymmetric CPW," *IEEE Trans. Antennas Propag.,* vol. 63, no. 2, pp. 760-765, February 2015.

[33] Y.-W.Zhong, G.-M. Yang, and L.-R. Zhong, "Gain enhancement of bow-tie antenna using fractal wideband artificial magnetic conductor ground," *Electronics Letters*, vol. 51, no. 4, pp. 315-317, February 2015.

[34] A. Dadgarpour, B. Zarghooni, B. S. Virdee, and T. A. Denidni, "Millimeter-wave high-gain SIW end-fire bow-tie antenna," *IEEE Trans. Antennas Propag.,* vol. 63, no. 5, pp. 2337-2342, May 2015.

[35] J. D. Kraus, "Antennas for all applications," McGraw-Hill, New York, 1988, 2 edn.

[36] Y. Mushiake, "Self-complementary antennas," *IEEE Antennas Propag. Mag.,* vol. 34, no. 9, pp. 23-29, December 1992.

[37] K. P. Ray, "Design aspects of printed monopole antennas for ultra-wide band applications," *Int. J. Antennas Propag.,* pp. 1-8, 2008.

[38] S. M. J. Razavi, D. Basaery, and S. H. Mohseni-Armaki, "Radiation pattern analysis of inverted-F antenna mounted on the side wall of a long cylinder," Journal of Communication Engineering, vol. 7, no 2, pp. 1-11, July-December 2018.

[39] C. A. Balanis, Antenna theory: Analysis and design, 2rd ed, Wiley, New York, 1997.

[40] Q. Wu, R. Jin, J. Geng, and M. Ding, "Pulse preserving capabilities of printed circular disk monopole antennas with different grounds for the specified input signal forms," *IEEE Trans. Antennas Propag.,* vol. 55, no. 10, pp. 2866–2873, October 2007.